

# Photosynthesis-Irradiance Relationship of Phytoplankton and Primary Production in the Vicinity of Kuroshio Warm Core Ring in Spring

KEN FURUYA<sup>1</sup>, OSAMU HASEGAWA<sup>1</sup>, TAKASHI YOSHIKAWA<sup>1</sup> and SATORU TAGUCHI<sup>2</sup>

<sup>1</sup>Department of Aquatic Bioscience, Graduate School of Agricultural and Life Sciences, The University of Tokyo, Bunkyo, Tokyo 113-8657, Japan

<sup>2</sup>Faculty of Engineering, Soka University, Tangi, Hachioji, Tokyo 192-0003, Japan

(Received 31 March 1998; in revised form 18 June 1998; accepted 22 June 1998)

The light-saturated maximum value ( $P^B_{\max}$ ) and initial slope ( $\alpha$ ) of the photosynthesis-irradiance (P-E) curve were examined in a warm streamer, a cold streamer and a warm core ring off the Sanriku area in the subarctic western North Pacific Ocean during an ADEOS/OCTS Sanriku field campaign in early May 1997. Both  $P^B_{\max}$  and  $\alpha$  were within the ranges of temperate populations. A regional difference was apparent in  $P^B_{\max}$ : populations in the warm streamer tended to show higher value ranging between 1.92 and 4.74 mgC (mgChl *a*)<sup>-1</sup>h<sup>-1</sup> than those in the cold streamer and the warm core ring (1.35–2.87 mgC (mgChl *a*)<sup>-1</sup>h<sup>-1</sup>). A depth variation was also observed in  $\alpha$  in both the warm streamer and the warm core ring: shallow populations tended to have lower  $\alpha$  than deep populations. The depth variations in both  $P^B_{\max}$  and  $\alpha$  resulted in a lower light intensity of the light saturation in a deeper population than that of a shallower one. These depth-related variations in the P-E parameters were likely a manifestation of “shade-adaptation” of photosynthesis. Photoinhibition was not observed over in situ surface light intensity varying below ca 1600  $\mu\text{mol photon m}^{-2}\text{s}^{-1}$ . Water-column primary productivity was bio-optically estimated to be 233 to 949 mgC m<sup>-2</sup>d<sup>-1</sup> using vertical distributions of the P-E parameters, chlorophyll *a*, phytoplankton light absorption and underwater irradiance. Applicability of surface data sets for estimation of water-column productivity is discussed.

Keywords:

- Photosynthesis,
- primary production,
- phytoplankton,
- P-E curve,
- subarctic Pacific,
- warm core ring,
- ADEOS/OCTS.

## 1. Introduction

Off Sanriku area in the subarctic western North Pacific Ocean is characterized by a complex distribution of water masses originating from Kuroshio and Oyashio, and by high eddy activities associated with generation of warm core ring (Yasuda *et al.*, 1992). Primary productivity in this region is therefore expected to be highly variable in time and space under the influence of the complex water-column physics (e.g. Kasai *et al.*, 1997). Existing knowledge about primary production in this area confirms its high variability (Saijo and Ichimura, 1960; Aruga *et al.*, 1968; Takahashi and Ichimura, 1972; Taniguchi and Kawamura, 1972; Hama, 1992; Shiomoto *et al.*, 1994; Shiomoto *et al.*, 1996). The variability is assigned to both phytoplankton biomass and photosynthetic activity. Chlorophyll *a* ranges over three orders of magnitude from <0.5 to >50 mg m<sup>-3</sup> off Sanriku, whereas the photosynthetic activity varies much less: for example assimilation index at the surface, in general, ranges between  $\approx 1$  and 10 mgC (mgChl *a*)<sup>-1</sup>h<sup>-1</sup>.

Photosynthetic rates are controlled by many factors.

Among them irradiance is the primary regulator. Dependence of photosynthesis on light can be analyzed with parameters of the photosynthesis-irradiance (P-E) relationship. The P-E curve is central in measuring, modeling, predicting phytoplankton photosynthesis, and evaluating physiological states of populations. However, data on the P-E curves such as light-saturated maximum rate and initial slope, are very scarce in the subarctic North Pacific, especially in the western part (Yokouchi *et al.*, 1997).

An extensive survey was conducted to investigate primary production and associated processes in off Sanriku area in May, 1997 with an emphasis on the utilization of ocean color information derived from Ocean Color and Temperature Scanner (OCTS) on board Advanced Earth Observing Satellite (ADEOS, otherwise known as Midori) (Kawamura, 1998). The present paper reports the P-E characteristics of phytoplankton during the survey. We also determine primary production bio-optically using the P-E parameters and environmental parameters.

## 2. Materials and Methods

Field experiments were carried out in a warm and cold streamer, and within a warm core ring during an ADEOS/OCTS Sanriku field campaign on board R/V *Tansei-Maru* (KT-97-05 cruise) on May 10 and 11, 1997 (Fig. 1). Water samples were taken using Niskin bottles mounted on a rosette sampler fitted with a multi-sensor array, OCTOPUS, which was equipped with a CTD (Niel Brown MKII), a  $4\pi$  photon collector (QSP-200, Biospherical) and a fluorometer (Aquatracka, Chelsea) (Ishimaru *et al.*, 1984). No metal part was used inside the bottles and attention was paid to avoid metal contamination throughout the handling of the seawater.

Photosynthetic rates of natural population were determined from uptake of  $\text{H}^{13}\text{CO}_3^-$  (Hama *et al.*, 1983). Samples collected from 2 or 4 depths were dispensed into 500-mL polycarbonate bottles, then added with about 10% enrichment of  $\text{NaH}^{13}\text{CO}_3$  of total inorganic carbon. Incubations were conducted for 2 h at ambient temperature under an artificial light gradient. A linear incubator capable of producing ca.  $1600 \mu\text{mol photon m}^{-2}\text{s}^{-1}$  light intensities was used with a halogen lamp as a light source. The color temperature of the light source was adjusted to ca  $5250^\circ\text{K}$  with an acrylic blue filter to simulate approximately the light quality of the surface water. Photosynthetic rates at 10 light levels including the dark control were obtained to construct a P-E curve. The incubator was cooled with a temperature-controlled water bath.

The incubations were terminated by filtering the samples onto 25-mm precombusted Whatman GF/F filters under a

gentle suction ( $<150 \text{ mmHg}$  negative pressure) under a dim light, followed by immediate freezing for later analysis on land. After removal of unfixed inorganic carbon with concentrated HCl fume, the filters were well dried in a vacuum desiccator. The isotopic ratio of  $^{13}\text{C}:^{12}\text{C}$  and particulate organic carbon were determined using a mass spectrometer (ANCA-SL, Europa Sci). Photosynthetic rates were corrected with time zero control. Total carbonate in the incubated water was measured with an infrared analyzer (TOC 5000 Shimadzu).

Photosynthetic rates were normalized to the concentration of chlorophyll *a*, and the hyperbolic tangent function (Jassby and Platt, 1976) was fitted to the data using the quasi-newton method to obtain P-E parameters: assimilation number ( $P^B_{\text{max}}$ ), i.e. plateau of the P-E curve, and the initial slope ( $\alpha$ ). Superscript B denotes photosynthetic rates normalized to chlorophyll *a*. The light adaptation index ( $E_k$ ; Talling, 1957), i.e. light intensity at the onset of saturation, was obtained from  $P^B_{\text{max}}$  and  $\alpha$  as  $E_k = P^B_{\text{max}}/\alpha$ .

Chlorophyll *a* concentration was determined fluorometrically (Turner Design, 10R) for particles collected on a Whatman GF/F glass fiber filter in the upper 37-m water column at Stn. 3, and in the upper 200 m at the other stations (Suzuki and Ishimaru, 1990). Samples for determining phytoplankton composition were fixed with 0.5% (v/v) buffered formalin, and used for microscopic observation. Temperature, salinity and underwater PAR field were measured using the OCTOPUS, and surface PAR was monitored at an average of every 10 minutes (Li-190S, LiCor). Light absorption of phytoplankton between 400 and 700 nm was measured spectrophotometrically (MPS-2000, Shimadzu) with 1-nm resolution on board ship for cells collected on GF/F filters by gentle suction using the opal glass method (Kishino *et al.*, 1985). The measurements were made in the upper 30- or 40-m water column (Saino and Goetz, 1997). Spectra of downward PAR was measured with a underwater spectroradiometer (MER2040, Biospherical; Saino and Goetz, 1997).

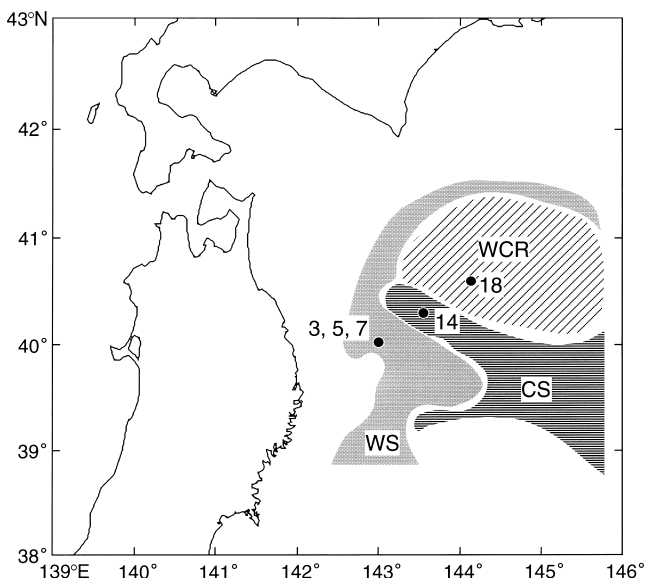


Fig. 1. Station locations. Stns. 3, 5 and 7 were located in a warm streamer (WS), Stn. 14 in a cold streamer (CS) and Stn. 18 in a Kuroshio warm core ring (WCR). Distributions of CS, WS and WCR are outlined based on consecutive infrared images of NOAA/AVHRR during the cruise.

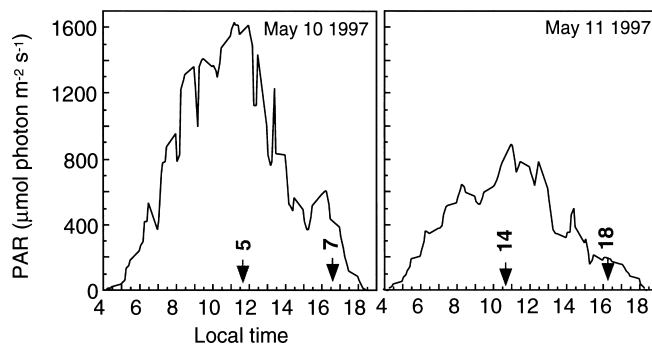


Fig. 2. Daily variations in the surface PAR on May 10 and 11, 1997. Sampling time is superimposed. Stn. 3 was sampled at midnight of May 10.

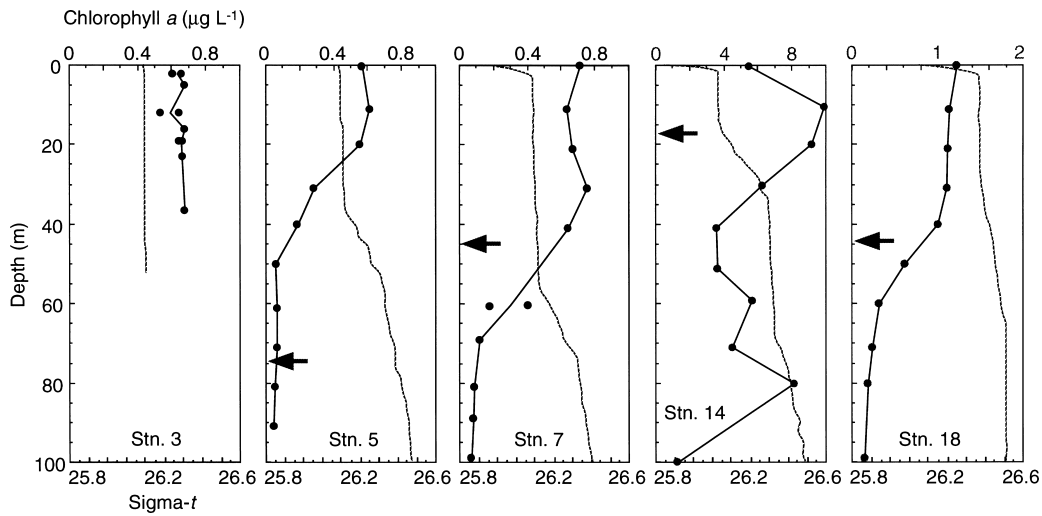


Fig. 3. Vertical distributions of chlorophyll *a* concentration (circle), and sigma-t (broken line). The depths of 1% light level of the surface are shown with arrows.

### 3. Results and Discussion

#### 3.1 Environmental conditions and phytoplankton distribution

A clear sky without cloud coverage was not obtained during the cruise. Surface PAR varied below  $1641 \mu\text{mol photon m}^{-2}\text{s}^{-1}$  in the vicinity of the Kuroshio warm core ring (Fig. 2). Chlorophyll *a* concentration near the surface was constant during a two days' stay in the warm streamer where nine vertical profiles were obtained, ranging between 0.6 and  $0.8 \mu\text{g L}^{-1}$  (Fig. 3). The highest concentration of chlorophyll *a* was observed in the cold streamer, reaching  $10 \mu\text{g L}^{-1}$  at 10-m depth. A subsurface maximum of chlorophyll *a* occurred around 80-m depth. Chlorophyll *a* concentration in the warm core ring was vertically uniform in the upper 40-m water column (Fig. 3). A regional difference was also apparent in the underwater light field (Fig. 3): the depth of 1% of the light level just above the surface was 73 m at Stn. 5, 45 m at Stn. 7, 17 m at Stn. 14 and 43 m at Stn. 18, inversely well correlated with integrated chlorophyll *a* amount in the upper layer above the 1% light depth, which is referred as the euphotic zone hereafter.

Chlorophyll-*a*-specific light absorption coefficient ( $a^*$ ) also differed among stations (Fig. 4). High absorption ( $>0.02$ ) was observed in the warm streamer where flagellates and monads were dominant (Waku and Furuya, 1998), while a population in the cold streamer mainly composed of diatoms exhibited low absorption from the surface to 30-m depth. Populations in the warm core ring showed intermediate absorption between those in the cold streamer and in the warm streamer. A distinct subsurface increase in  $a^*$  was observed at Stn. 5.

Chlorophyll-*a*-specific light absorption of phytoplankton averaged for 400-700 nm ( $\text{m}^2 [\text{mg chl } a]^{-1}$ )

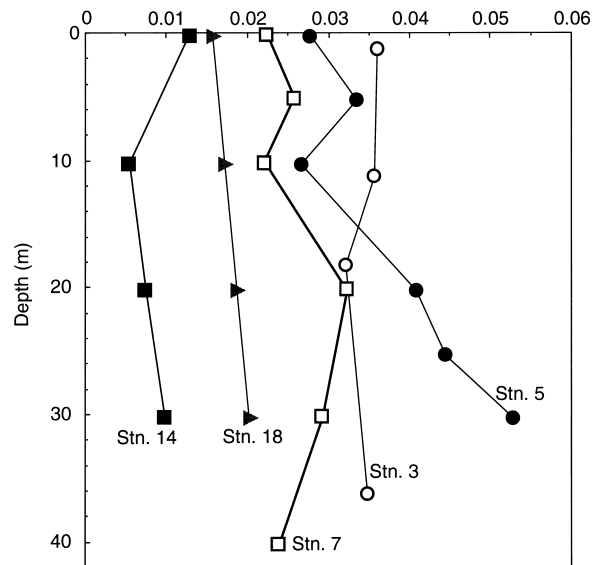


Fig. 4. Vertical distributions of chlorophyll-*a*-specific light absorption of phytoplankton averaged over wavelength between 400 and 700 nm.

#### 3.2 P-E parameters

No sample exhibited photoinhibition over the light intensity of 0 to  $1600 \mu\text{mol photon m}^{-2}\text{s}^{-1}$  (Fig. 5). The range corresponded approximately to daily irradiance at the sur-

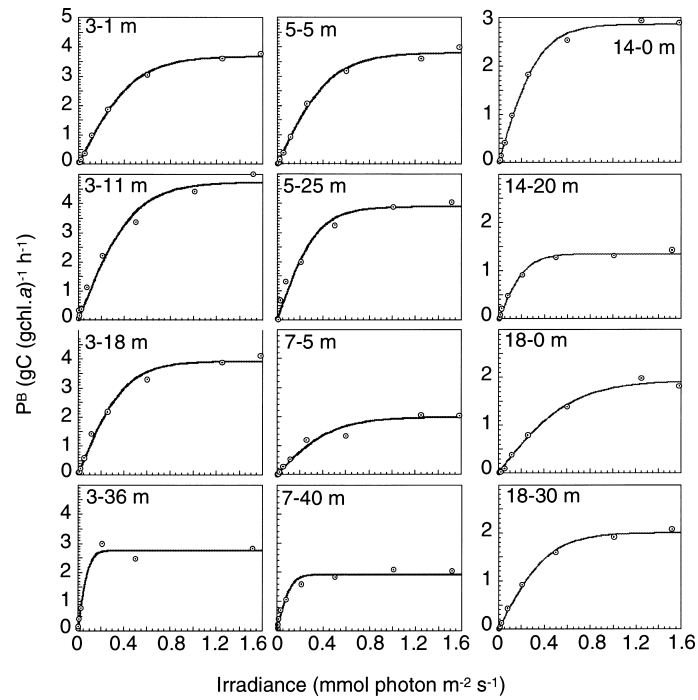


Fig. 5. Photosynthesis versus irradiance relationships. Photosynthetic rates were normalized to chlorophyll *a* (denoted by superscript B). Line fitting was made to hyperbolic tangent function (Jassby and Platt, 1976) using the quasi newton method.

Table 1. Summary of parameters for photosynthesis-irradiance curves. Underwater PAR relative to that just above the surface is also given.

Station	Depth (m)	Relative light intensity (%)	Initial slope ( $\alpha$ ) $\times 10^{-3} \text{ mgC (mgChl } a)^{-1} \text{ h}^{-1}$ $(\mu\text{mol photon m}^{-2} \text{ s}^{-1})^{-1}$	Maximum photosynthetic rate ( $P_{\text{max}}^B$ ) $\text{mgC (mgChl } a)^{-1} \text{ h}^{-1}$	Onset of light saturation ( $E_k$ ) $\mu\text{mol photon m}^{-2} \text{ s}^{-1}$
3	1	nd	7.71	3.69	479
	11	nd	10.0	4.74	474
	18	nd	9.79	3.93	401
	36	nd	31.5	2.76	88
5	5	45.6	8.25	3.80	461
	25	11.4	11.4	3.89	341
7	5	34.4	4.06	1.98	488
	40	1.5	17.2	1.92	112
14	1	71.9	8.08	2.87	355
	20	0.5	5.68	1.35	238
18	1	79.5	3.07	1.93	629
	30	3.3	4.60	2.01	437

nd: no data.

face (Fig. 2). The hyperbolic tangent function was then applied to obtain the P-E parameters (Table 1). Both  $P_{\max}^B$  and  $\alpha$  were within the ranges of temperate population (Harrison and Platt, 1986). A regional difference was apparent in  $P_{\max}^B$ . Populations in the warm streamer tended to show higher maximum photosynthesis than those in the cold streamer and the warm core ring. The variability was also observed within the warm streamer:  $P_{\max}^B$  near the surface Stns. 3 and 5 was approximately twice of that at Stn. 7.  $E_k$  at the surface varied between 355 and 629  $\mu\text{mol photon m}^{-2} \text{s}^{-1}$ , considerably higher than the median value of 216  $\mu\text{mol photon m}^{-2} \text{s}^{-1}$  as examined for temperate populations (Harrison and Platt, 1986).

A depth variation was also observed in the initial slope at most stations. Shallow samples tended to have lower  $\alpha$  than deep populations except Stn. 14 (Fig. 5). This was most apparent in the warm streamer: the population taken at 36-m depth at Stn. 3 had an enhanced initial slope compared to those in the upper layer (Table 1). This suggested the population at 36 m had been optically isolated from the upper population for some period, long enough to allow an adaptation to the low light. However, there was no indication supporting the vertical separation of the near surface population from subsurface populations: no density structure was obvious in the upper 40-m water column, and phytoplankton composition was vertically uniform (Waku and Furuya, 1998). At present, further information on the vertical mixing rate of the water column will be needed to explain the vertical difference in  $\alpha$ . On the other hand there was a weak pycnocline between the “shallow” and the “deep” samples at 16-m depth of Stn. 5 and at 20, 30 and 38 m at Stn. 7, likely causing a photoadaptation of the “deep” population to weak light field at these stations. Although the subsurface increase of  $\alpha$  was common in the warm streamer (Table 1), cellular physiology seemed to vary among stations: the increase in  $a^*$  was observed only at Stn. 5, and this likely reflected higher light harvesting capacity in the subsurface population at Stn. 5 than those at other stations, although supporting evidence for this inference, such as pigment composition, is not available at present.

While  $P_{\max}^B$  showed relatively less variability with depth than  $\alpha$ , samples taken from the bottom of the euphotic zone at Stns. 3 and 14 showed lower rate than in the upper layer. Despite the various changes in both  $P_{\max}^B$  and  $\alpha$ , their depth variations produced a lower  $E_k$  in a deeper sample than that of a shallower one at all stations (Table 1). These depth-related variations in the P-E parameters were likely a manifestation of “shade-adaptation”.

Since seawater was taken at various times of the day (Fig. 2), our measurements of photosynthetic rates might include some influence of possible diurnal physiological rhythm. However, this possibility was not examined in the present study, in which different water masses were taken at each sampling.

### 3.3 Primary production

Primary productivity was estimated based on the spectral model of Morel (1991) using the observed values of chlorophyll *a*, downward irradiance, chlorophyll-*a*-specific light absorption coefficient and the P-E parameters. Daily primary production at depth *z* ( $P(z)$ ) can be obtained as follows:

$$P(z) = \int_0^D f\left(\int_{\lambda_1}^{\lambda_2} PAR(\lambda, z, t) d\lambda\right) \times B(z, t) dt \quad (1)$$

where  $B(z, t)$  is chlorophyll *a* concentration at depth *z* and time *t* ( $\text{mg m}^{-3}$ ),  $PAR(\lambda, z, t)$  is PAR of wavelength  $\lambda$  at depth *z* and time *t* ( $\text{mol photon m}^{-2} \text{s}^{-1} \text{nm}^{-1}$ ), *D* is length of daytime (s),  $\lambda_1$  and  $\lambda_2$  are the shorter and longer end of PAR, 400 and 700 nm, respectively, and the function *f* expresses the  $P^B$ -E relationship. Here, we use the hyperbolic tangent function for the function *f*. Since the function *f* depends on wavelength, we considered photosynthetically usable radiation and a function *g* is introduced which is linearly transformed from the function *f* as

$$g\left(PAR \times a^*(\lambda, z, t)\right)\Big|_{z=0} = f(PAR)\Big|_{z=0} \quad (2)$$

where  $a^*(\lambda, z, t)$  is chlorophyll *a*-specific light absorption coefficient of wavelength  $\lambda$  at depth *z* and time *t* ( $\text{m}^2[\text{mgChl } a]^{-1} \text{nm}^{-1}$ ). Here, we assume the shape of the action spectrum of  $\alpha$  is same as that of  $a^*$  at the surface (Morel, 1991). Then Equation 1 can be rewritten with the transformation (2) as:

$$P(z) = \int_0^D g\left(\int_{\lambda_1}^{\lambda_2} PAR(\lambda, z, t) \times a^*(\lambda, z, t) d\lambda\right) \times B(z, t) dt. \quad (3)$$

$B(z, t)$  and  $a^*(\lambda, z, t)$  were calculated at a 1-m depth interval by linear interpolation from the observed vertical data (Figs. 3 and 4), and constant values of  $a^*(\lambda, z_{\text{deepest}}, t)$  was used below the deepest observed layer ( $z_{\text{deepest}}$ ). The  $z_{\text{deepest}}$  was from 30- to 40-m (Fig. 4).  $B(z, t)$  and  $a^*(\lambda, z, t)$  were assumed to be constant with time. The  $P^B$ -E parameters at every meter were determined as follows: For example, at Stn. 5 the parameters obtained at 5-m depth were used for 0 to 5-m depths, and those between 6- and 24-m depths were linearly interpolated from measured values of 5- and 25-m depths. Values for >25-m depths were supposed to be equal to those at 25 m.  $PAR(\lambda, z, t)$  was calculated at a 1-nm wavelength resolution by linear interpolation from observed spectra of downward PAR, assuming that temporal fluctuation of  $PAR(\lambda, 0, t)$  was same as that of the surface PAR. The surface PAR on May 10 was applied to the calculation (Fig. 2). Thus, the calculation was made at a 1-m interval vertically, 1-nm in wavelength, and 10 minutes temporarily.

Thick lines in each panel in Fig. 6 illustrate the vertical

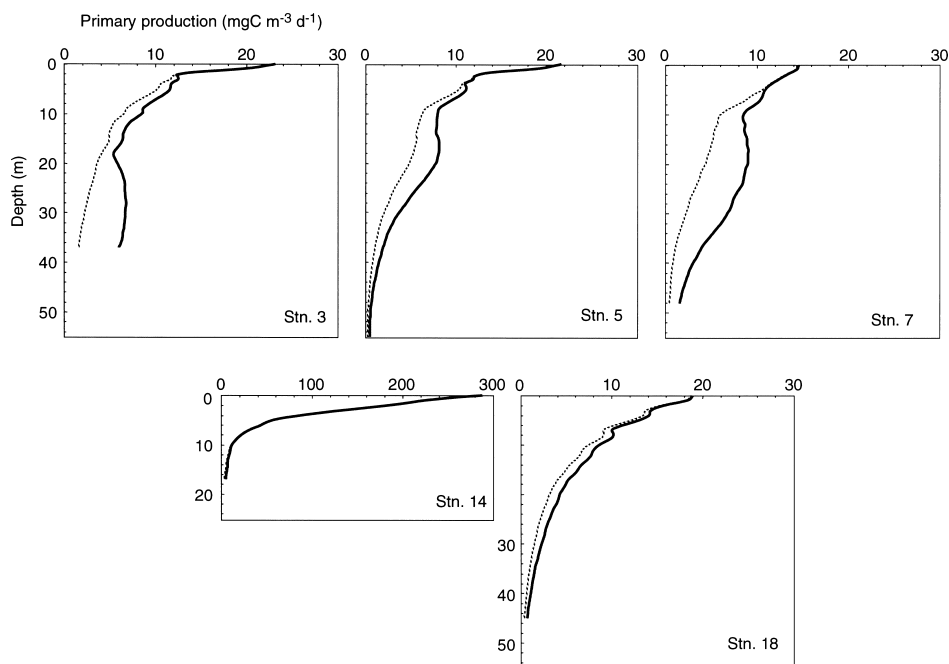


Fig. 6. Bio-optically derived primary production. Thick lines denote primary production calculated using linearly interpolated P-E parameters. Profiles shown with broken lines were obtained with near-surface P-E parameters applied throughout the water column. For details, see text.

Table 2. Integrated daily primary production in the vicinity of a Kuroshio warm core ring in May 1997. Results of three different calculations are given: (1) calculation using two or four P<sup>B</sup>-E parameter sets (Combined), (2) conventional chlorophyll method (Conventional), (3) calculation using the shallowest parameter set for the whole water column (Shallow). Chlorophyll *a*-based productivity is also given for "Combined" production.

Station	Depth range (m)	Primary production (mgC m <sup>-2</sup> d <sup>-1</sup> )			Primary productivity (mgC [mgChl <i>a</i> ] <sup>-1</sup> d <sup>-1</sup> )
		Combined	Conventional	Shallow	Combined
3	0–37	287	251	197	11.9
5	0–73	278	190	213	13.2
7	0–48	333	236	200	10.5
14	0–17	949	1401	972	6.72
18	0–45	233	201	203	4.73

profiles of daily primary production. Figure 6 also shows profiles with finer lines which represent daily primary production based on the near-surface P-E parameter data set applied to the whole water column. Vertical distribution of daily primary production was highest at the surface, and decreased rapidly with depth. This demonstrates the importance of surface samples in determining primary production. The subsurface enhancement of productivity was obvious compared to the profiled based on the near-surface P-E parameters. This was largely due to higher *a* in the depths (Table 1 and Fig. 5).

Water-column primary productivity ranged from 233

to 949 mgC m<sup>-2</sup>d<sup>-1</sup> ("Combined" in Table 2). The integration was made along the thick lines in Fig. 6 from the surface down to 37-m depth at Stn. 3 and to the bottom of the euphotic zone at other stations. These estimates were within the ranges of reported spring values off Sanriku area (e.g. Saijo and Ichimura, 1960; Aruga *et al.*, 1968; Takahashi and Ichimura, 1972; Taniguchi and Kawamura, 1972; Shiimoto *et al.*, 1994, 1996, 1998). Chlorophyll-*a*-based integrated productivity was higher in the warm streamer than in the cold streamer and the warm core ring (Table 2). These figures confirm the regional variability of photosynthetic activity (Fig. 5, Table 1). Since daily primary production

varies according to temporal fluctuation of surface irradiance, our estimates based on that of May 10 are only tentative. However, the daily insolation of 38.1 mol photon  $\text{m}^{-2}$  on May 10 was close to spring mean of the area (Hirotaka Otake, personal communication), and our estimates are considered to represent production in spring.

The highest production at Stn. 14 was primarily owing to high phytoplankton biomass and not to enhanced photosynthetic activity (Fig. 3 and Table 1). Since chlorophyll *a* often exceeds 20  $\text{mg m}^{-3}$  during spring bloom in the water influenced by Oyashio (e.g. Harashima and Kikuchi, 1991; Kasai *et al.*, 1997), primary production can be expected to reach more than double our estimates in spring. A clear dependence of the integrated production on chlorophyll *a* abundance is confirmed during the field campaign (Ishizaka, 1998). Daily primary production from the surface to 35-m depth was also estimated to be 214  $\text{mgC m}^{-2}\text{d}^{-1}$  in the vicinity of Stn. 3 from  $^{13}\text{C}$  uptake based on an in situ 24 h incubation on May 10 and 11, 1997 (Saino and Goetz, 1997). In our estimation daily production in the warm core ring varied between 278 and 333  $\text{mgC m}^{-2}\text{d}^{-1}$  with a mean of 299  $\text{mgC m}^{-2}\text{d}^{-1}$  (Table 2). Thus, the present calculation yielded 40% greater production than the in situ uptake. The difference was probably ascribable, in part, to the incubation time: our estimates with much shorter duration was considered to be closer to gross production, while that of the in situ experiment approximates net primary production.

The estimates were compared with those of conventional "chlorophyll method", which does not take light absorption of phytoplankton into account; that is,  $PAR(\lambda, z, t)$  in Eq. (1) was replaced by total PAR between 400 and 700 nm (Table 2). Both in the warm streamer and the warm core ring the bio-optical model which considers  $a^*$  gave higher estimates than the chlorophyll method by 13 to 32%, 22% on average. By contrast, the chlorophyll method resulted in a higher value than the model at Stn. 14. Thus, primary production derived from the bio-optical model revealed that effects of phytoplankton absorption were opposed between the warm streamer and the cold streamer (Table 2). In any case the difference between the two methods was 48% at most.

The shade adaptation of the P-E parameters contributed to subsurface enhancement of primary productivity both in the warm streamer and the warm core ring (Fig. 6). When the shallowest P-E parameters were applied to the whole water column as denoted by broken lines in Fig. 6, integrated production was underestimated by 13 to 40% in both these waters ("Shallow" in Table 2). Thus, the application of surface parameters can result in the underestimation with shade adapted subsurface populations. On the contrary the "Shallow" integration gave a slight overestimation at Stn. 14. The difference of the "Shallow" integration from the "Combined" one was from +2 to -40% of the "Combined" estimation. The maximum uncertainty goal for OCTS data

is 30% for chlorophyll *a* in case-1 waters (National Space Development Agency of Japan, 1995). The possible errors introduced by the "Shallow" estimation was of a similar magnitude. Furthermore, a tentative calculation using surface  $a^*$  for the whole euphotic zone instead of the vertical  $a^*$  data gave 7 to 27% of deviation from the "Combined" production. Therefore, although our observations are limited in number, use of the surface P-E parameters or  $a^*$  did not result in a serious errors in the estimation of the integrated primary production. Consequently, an extensive survey for the bio-optical parameters at the surface should be emphasized for determining primary productivity from ocean color data.

### 3.4 Concluding remarks

The present study has demonstrated regional differences in both  $\alpha$  and  $P_{\text{max}}^B$  off Sanriku area and confirms that they were within the reported ranges for the temperate population, but were relatively high. Since the amplitude of seasonal variations in the P-E parameters is reported to be high in the area (Yokouchi *et al.*, 1997), investigations in the other seasons will be a next step for establishment of the data base in the area.

The P-E parameters obtained in the present study will serve as basic information in a local algorithm for estimating primary production based on ocean color. However, the area is known for its frequent, extended cloud coverage, especially during spring. Therefore, ocean color data can be acquired only on fine days. As a result primary production derived from ocean color may tend to be higher than the real value (Ishizaka, 1998). Thus shipborne observations together with parallel use of buoy sensors are a prerequisite for robust interpretations of remotely sensed primary production.

### Acknowledgements

We thank all the participants of the KT-97-05 cruise for their collaboration at sea. NOAA/AVHRR images of sea surface temperature prepared by S. Saito were very useful. We are also grateful to I. Koike and T. Hasegawa for their generous cooperation in mass spectrometry.

### References

- Aruga, Y., Y. Yokohama and M. Nakanishi (1968): Primary productivity studies in February–March in the northwestern Pacific off Japan. *J. Oceanogr. Soc. Japan*, **24**, 275–280.
- Hama, T. (1992): Primary productivity and photosynthetic products around the Kuroshio warm core-ring. *Deep-Sea Res.*, **39**, S280–S293.
- Hama, T., Y. Miyazaki, Y. Ogawa, T. Iwakuma, M. Takahashi, A. Otsuki and S. Ichimura (1983): Measurement of photosynthetic production of a marine phytoplankton population using a stable  $^{13}\text{C}$  isotope. *Mar. Biol.*, **73**, 31–36.
- Harashima, A. and Y. Kikuchi (1991): Sea truth database for satellite chlorophyll analysis and its quasi-3D graphics. *Kohsuiken Note*, **13**, 9–14 (in Japanese).

- Harrison, W. G. and T. Platt (1986): Photosynthesis-irradiance relationships in polar and temperate phytoplankton populations. *Polar Biol.*, **5**, 153–164.
- Ishimaru, T., H. Otake, H. Hasumoto and T. Nakai (1984): OCTOPUS, an octoparameter underwater sensor, for use in biological oceanography studies. *J. Oceanogr. Soc. Japan*, **40**, 207–212.
- Ishizaka, J. (1998): Spatial distribution of primary production off Sanriku, northwestern Pacific, during spring estimated by Ocean Color and Temperature Scanner (OCTS). *J. Oceanogr.*, **54**, this volume, 553–564.
- Jassby, A. D. and T. Platt (1976): The relationship between photosynthesis and light for natural assemblages of coastal marine phytoplankton. *J. Phycol.*, **12**, 412–430.
- Kasai, H., H. Saito, A. Yoshimori and S. Taguchi (1997): Variability in timing and magnitude of spring bloom in the Oyashio region, the western subarctic Pacific off Hokkaido, Japan. *Fish. Oceanogr.*, **6**, 118–129.
- Kawamura, H. (1998): OCTS mission overview. *J. Oceanogr.*, **54**, this volume, 383–399.
- Kishino, M., M. Takahashi, N. Okami and S. Ichimura (1985): Estimation of the spectral absorption coefficients of phytoplankton in the sea. *Bull. Mar. Sci.*, **37**, 634–642.
- Morel, A. (1991): Light and marine photosynthesis: a spectral model with geochemical and climatological implications. *Prog. Oceanogr.*, **26**, 263–306.
- National Space Development Agency of Japan (1995): *ADEOS Reference Handbook*. 332 pp. National Space Development Agency of Japan, Tokyo.
- Saijo, Y. and S. Ichimura (1960): Primary production in the Northwestern Pacific Ocean. *J. Oceanogr. Soc. Japan*, **16**, 139–145.
- Saino, T. and H. Goetz (1997): *Preliminary data report of the cruise KT-97-05 for the ADEOS Field Campaign*. Institute for Hydrospheric-Atmospheric Sciences, Nagoya University, 35 pp.
- Shiomoto, A., K. Sasaki and S. Shimada (1996): Primary production and contribution of “new” production in the warm core ring and the cold streamer off Sanriku in May 1990. *La mer*, **34**, 1–9.
- Shiomoto, A., S. Hashimoto and T. Murakami (1998): Primary productivity and solar radiation off Sanriku in May 1997. *J. Oceanogr.*, **54**, this volume, 539–544.
- Shiomoto, A., K. Sasaki, S. Shimada and S. Matsumura (1994): Primary productivity in the offshore Oyashio in spring and summer 1990. *J. Oceanogr.*, **50**, 209–222.
- Suzuki, R. and T. Ishimaru (1990): An Improved method for the determination of phytoplankton chlorophyll using N,N-Dimethylformamide. *J. Oceanogr. Soc. Japan*, **46**, 190–194.
- Takahashi, M. and S. Ichimura (1972): Some aspects of primary production in the northwestern Pacific Ocean. p. 218–229. In *Biological Oceanography of the Northern North Pacific Ocean*, ed. by A. Y. Takenouchi *et al.*, Idemitsu Shoten, Tokyo.
- Talling, J. F. (1957): The phytoplankton population as a compound photosynthetic system. *New Phytol.*, **56**, 133–149.
- Taniguchi, A. and T. Kawamura (1972): Primary production in the Oyashio region with special reference to the subsurface chlorophyll maximum layer and phytoplankton-zooplankton relationships. p. 231–243. In *Biological Oceanography of the Northern North Pacific Ocean*, ed. by A. Y. Takenouchi *et al.*, Idemitsu Shoten, Tokyo.
- Waku, M. and K. Furuya (1998): Primary production and community respiration in a warm streamer associated with Kuroshio warm core ring in spring. *J. Oceanogr.*, **54**, this volume, 565–572.
- Yasuda, I., K. Okuda and M. Hirai (1992): Evolution of a Kuroshio warm core ring: variability of the hydrographic structure. *Deep-Sea Res.*, **39**, S131–S161.
- Yokouchi, K., A. Tomosada and Y. Matsuo (1997): Photosynthesis-light response curves in Kuroshio, Oyashio and the transition area off Tohoku. *Bull. Tohoku Natl. Fish. Res. Inst.*, **59**, 127–138.